MODELING AND TRANSIENT ANALYSIS OF A NOVEL ADSORPTION CYCLE CONCEPT FOR SOLAR COOLING

Valentin Schwamberger[1], Christian Glück[1] and Ferdinand P. Schmidt[1,2]

[1] Karlsruhe Institute of Technology, Institute of Fluid Machinery, Karlsruhe (Germany),

[2] Fraunhofer Institute for Solar Energy Systems, Freiburg (Germany)

1. Introduction

When solar cooling is employed to generate chilled water utilizing heat from non-tracking solar thermal collectors to drive the thermodynamic cycle, there commonly is a choice between single stage absorption or adsorption chillers. In most installations realized to date, absorption chillers have been chosen due to their superior coefficient of performance (COP) and lower investment costs (see e.g. Henning, 2007).

This paper reports on a way to improve the COP of adsorption chillers to make them competetive with their absorption counterparts while avoiding some of the limitations of the latter. As has been pointed out by Cerkvenik et al. (2001), the cycling of inert mass and incomplete heat recovery between adsorbers are the key factors that lead to a lower COP of adsorption chillers compared to absorption ones. Therefore it is mainly the lack of an equivalent to the solution heat exchanger that limits the COP of the adsorption cycle. The idea of the cycle analyzed here is that instead of employing multiple adsorbers to improve heat recovery, the heat recoverable during adsorption could be stored at many temperature levels within a stratified thermal storage until needed for the next desorption half cycle. This cycle concept named “Stratisorp” was first presented by Schmidt et al. (2007), patent applications are pending (Munz et al., 2009). A thermodynamic analysis of the cycle for the case of a high temperature system with zeolite 13 X and thermal oil as heat transfer fluid has been presented by Schwamberger et al. (2011, 2011a).

2. The Stratisorp system

Fig. 1 shows the system operation schematically for the adsorption phase. In its simplest configuration considered here, the system requires only one adsorber. The temperature of the heat transfer fluid (HTF) in the storage rises monotonically from the heat rejection temperature T_{reject} at the bottom to the maximum regeneration temperature T_{reg} at the top. The adsorber is supplied with HTF extracted from the storage only.

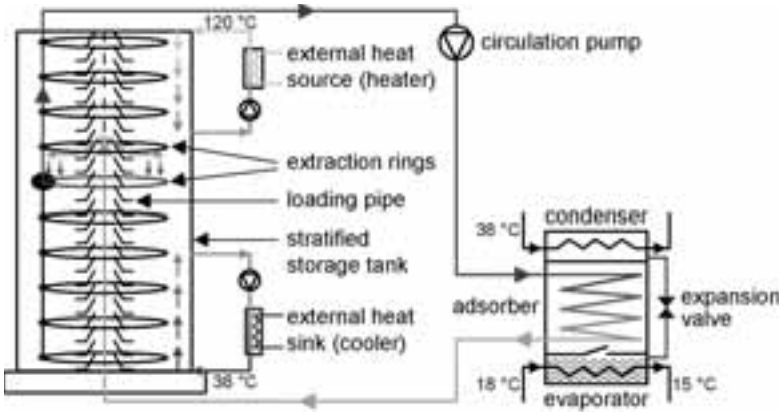

Fig. 1: Schematics of the Stratisorp system in the adsorption half cycle. The large black bullet indicates the ring used for fluid extraction; arrows at the loading pipe denote the fluid inserted into the tank.

The driving heat is supplied directly to the storage by an auxiliary heater connected to an external heat source. Equivalently, the excess heat at lower temperatures is removed by a cooler connected to the cooling tower. Both devices are integrated into the storage and may operate continuously over the cycle, since the storage is used as a buffer. During adsorption, HTF is extracted from the storage at the highest level

(indicated in Fig. 1 by a black bullet) whose temperature is lower by some ΔT_{set} than that of the fluid within the adsorber. When the fluid temperature difference falls below this value, a multi-way valve (not shown) is used to select the next lower extraction ring. The HTF is heated up in the adsorber and then reinserted into the storage via a concentric loading pipe. Due to the density gradient in the storage, the HTF leaves the pipe at a height corresponding to its temperature, and the thermal stratification is preserved. Such stratification devices are known from solar thermal systems (cf. Andersen et al., 2008), but they may have to be adapted to different flow rates and temperature conditions. During desorption, fluid is extracted at increasingly higher levels from the storage, again controlled by comparing the fluid temperature difference to ΔT_{set}.

The fraction of heat recoverable in this way depends primarily on the external temperature conditions and the adsorption equilibria of the selected working pair (e.g. zeolite/water), on the inert mass and heat transfer properties of the adsorber and on the exergy loss through mixing and energy loss (heat transfer to the surroundings) of the storage vessel.

For solar cooling of buildings with non-tracking collectors, suitable water adsorbents are silica gels or novel crystalline adsorbents such as SAPO-34, which shows a high water adsorption capacity with an S-shaped adsorption isotherm and is marketed by Mitsubishi Chemicals under brand name FAM-Z02 (Kakiuchi et al., 2005). In this simulation study, SAPO-34 is considered as adsorbent. With regards to the adsorber, a novel high-performance design that is currently under development at Fraunhofer ISE and Karlsruhe Institute of Technology (Wittstadt et al., 2009) has been considered here. It is based on extruded flat pipes as fluid channels (2 mm channel height) soldered to a composite of sintered metal fibers and SAPO-34. The adsorbent/matrix mass ratio and heat conductivity assumed here are consistent with laboratory values achieved on small samples with the same adsorbent (Füldner et al., 2011). In principle, the Stratisorp cycle could be realized with any adsorber, but since the driving temperature differences between fluid and adsorbent are small compared to the standard two-adsorber cycle, the power from standard packed-bed adsorbers would be very low, leading to long cycle times and thus to high mixing and heat losses from the storage.

The system is designed for a cooling power of 10 kW, leading to 20 kg of adsorbent (157 kg adsorber mass, 10 kg mass of piping, $U(T) \cdot A \approx 55$ kW K^{-1} for the heat transfer between HTF and adsorbent) and a storage fluid mass of 500 kg. Since we consider a single-adsorber system in our model, the evaporator is equipped with a 400 kg pool of water to prevent freezing during adsorption and to provide a buffer storage for the desorption phase ($U \cdot A = 8$ kW K^{-1} for condenser and evaporator).

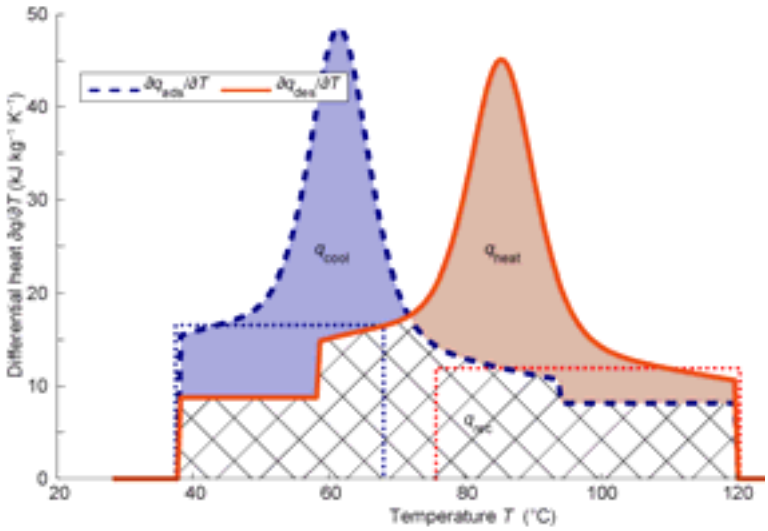

Fig. 2: Differential heat curves based on adsorption equilibria for the adsorption pair SAPO-34/water at 18 °C evaporator temperature, 38 °C condenser temperature and 120 °C regeneration temperature.

3. Stationary analysis

In Fig. 2, the differential heat curves for adsorption and desorption based on adsorption equilibria and adsorber configuration are shown. Adsorption equilibria have been parameterized using Dubinin's 'characteristic curve' with arbitrary fit functions, as introduced by Núñez et al. (1999). Cycle temperatures are 120 °C for regeneration, 38 °C for heat rejection and 18 °C evaporator temperature. Heat released during adsorption is shown as dashed line, heat supplied during desorption as solid line. The crisscrossed area corresponds to the recoverable heat. It can be seen that besides the sensible heat, some of the sorptive heat can be recovered. The COP for ideal heat recovery is 1.19 under these conditions. The dotted rectangle in the high temperature range indicates the largest possible temperature spread of an external fluid heating loop that heats fluid plugs extracted from the system at some extraction temperature, to be reinserted at maximum regeneration temperature (i.e., heating at constant differential heat if temperature independent heat capacity of fluid is assumed). In the same way, the dotted rectangle on the low temperature side represents the largest possible temperature spread of an external cooler.

In order to estimate the potential for heat recovery for a system operated at finite cooling power, a driving temperature difference between fluid and adsorber can be considered in calculating the differential heat curves. This situation is shown in Fig. 3 for a driving temperature difference of 5 K during adsorption and desorption.

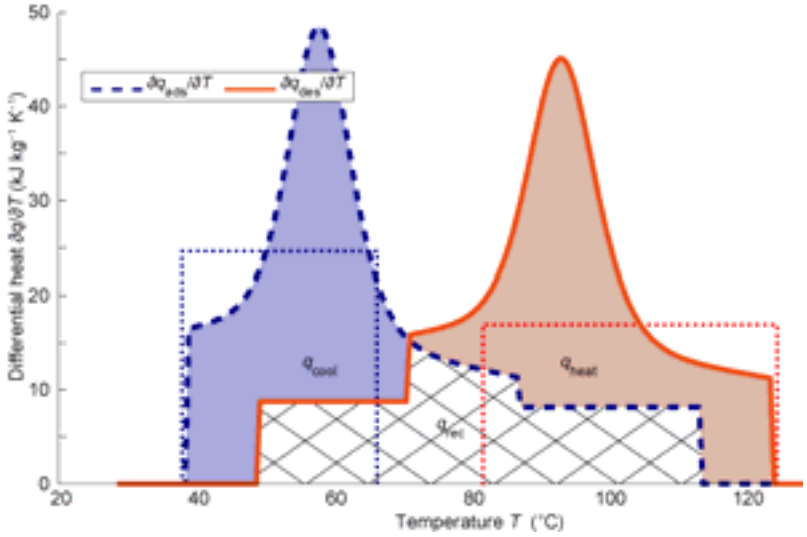

Fig. 3: Differential heat curves as in Fig. 2, but including an assumed driving temperature difference of 5 K between adsorbent and fluid both in adsorption and desorption mode.

It can be seen that the recoverable heat is strongly reduced, but still some sorptive heat can be recovered. If q_{rec} is completely recovered, the COP is 0.85 in this case.

4. System model for transient simulations

The dynamic model has been implemented in MATLAB®. It can be divided into the adsorber model and the storage model. The fluid flow between the storage and the adsorber is modeled as an ideal plug flow.

The one-dimensional adsorber model consists of a number of temperature nodes (default: 32) that comprise the heat exchanger and the adsorbent. Each of them interacts with the corresponding fluid plug and with its two adjacent adsorber nodes: The heat transfer between the fluid and the adsorber nodes is computed via an NTU model. Additionally, pipe nodes that represent the thermal mass of the pipings that do not belong to the adsorber (connections between adsorber elements, inlets and outlets) are accounted for. Adsorption and desorption of vapor is computed with the help of Dubinin's theory (Núñez et al., 1999) for every adsorber node separately, since it is dependent on the current temperature of respective node. The same applies for the adsorption enthalpies.

Condenser and evaporator have been modeled with single node NTU models. The respective heat exchanger receives heat from the cold supply loop (evaporator) or transfers heat to the heat rejection loop (condenser). For the adsorber nodes as well as evaporator and condenser, a system of coupled differential equations for the loading, the pressure, and the temperature is integrated over the duration of each plug flow time step. During the isosteric phases of the cycle when all valves between adsorber and evaporator/condenser are closed, the adsorber can exchange loading with a vapor chamber. This commonly leads to a redistribution of adsorbate between adsorber nodes depending on the temperature gradient during the isosteric phase.

The storage model is also one-dimensional: The height of the storage is discretized into a number of layers (about 1000). The extraction through the rings (default: 15 rings), the reinsertion through the loading pipe as well as the extractions and insertions related to the cooler and the heater are performed ideally in every time step. Due to the differing volume flows in the adsorber and heater/cooler loops, a fractional plug flow model has been implemented. After each plug flow time step, a mixing step is conducted to account for all heat transfer effects in the storage aside from the ideal plug flow (convection and conduction): At each inlet or outlet, the actual heat conductivity of the fluid k is increased by an amplification factor (default value: 100). Around the peak, it continues like a Gaussian function (default width: 5 % of the storage height for all inlets and outlets except the loading pipe, where we assumed 10 % of the storage height as default width and a default amplification factor of 50). These assumptions are somewhat arbitrary since they have not been checked experimentally yet. One would expect the amplification factor to depend on the mass flow, which is not the case in our model yet. Some preliminary CFD results suggest that the order of magnitude of the mixing effects is correct, experimental investigations are underway. From a solar cooling application perspective, it is clear that mixing effects in the storage could be reduced quite easily by using porous media such as reticulated foams to suppress both large scale eddies and turbulence. The storage content is 500 kg of fluid, and the height of the cylindrical storage is 1.9 m, with 25 cm of insulation (k = 0.04 W/(m K)).

The operating strategy is based on the mass flow ratios between the adsorber fluid loop (denoted as system mass flow) and all other loops. Hence, altering the system mass flow for adapting the power output of the system changes the other mass flows simultaneously, leading to a near-constant temperature spread over the cycle if desired.

5. Simulation results

For each configuration and set of operating conditions, the transient system behavior is simulated until stationary cycles are reached. The temperatures and loadings of the stationary cycle are shown in Fig. 4.

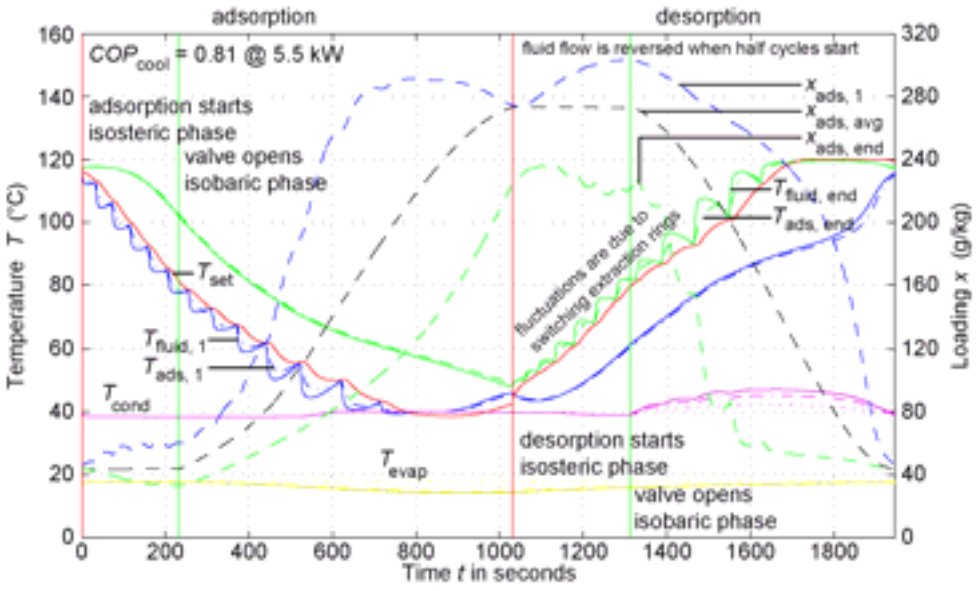

Fig. 4: Temperatures (left axis) and adsorbate loadings (right axis) over a complete cycle. External temperatures are 120 °C (regeneration), 18 °C (evaporator supply), and 38 °C (condenser/adsorber cooling supply).

The external temperatures are set to 120 °C (regeneration), 38 °C (supply to dry cooling tower, i.e. assumed air temperature) and 18 °C (evaporator supply, e.g. from a chilled ceiling). These temperatures are taken as the base case for all parameter variations. The system mass flow is 0.4 kg/s, leading to a cooling power of 5.5 kW (i.e. a part load state for a system with 10 kW design power) and a COP of 0.81. The heater and cooler extraction heights have been set to 75% and 25% of the storage height, respectively. The heater and cooler mass flows are set to 35% of the system mass flow.

It can be seen from Fig. 4 that in the adsorption phase, the cooling of the adsorber is insufficient to achieve full adsorption of the SAPO-34, resulting in a large loading spread between adsorber nodes at the end of the adsorption phase, and to a strong redistribution of adsorbate in the following isosteric phase.

Storage results

The storage can be looked at in two different ways: with a focus on spatial or temporal resolution. Fig. 5 shows the temperature profile of the storage averaged over a complete cycle (central line) along with the intervals of one and two standard deviations from the mean values (shaded areas). The temperature profiles at the end of each half cycle are plotted as dotted lines. It can be seen that the temperature profile is approximately linear and the temperature spread between adsorption and desorption is about 20 K in the central region of the tank between the heater and cooler extraction levels.

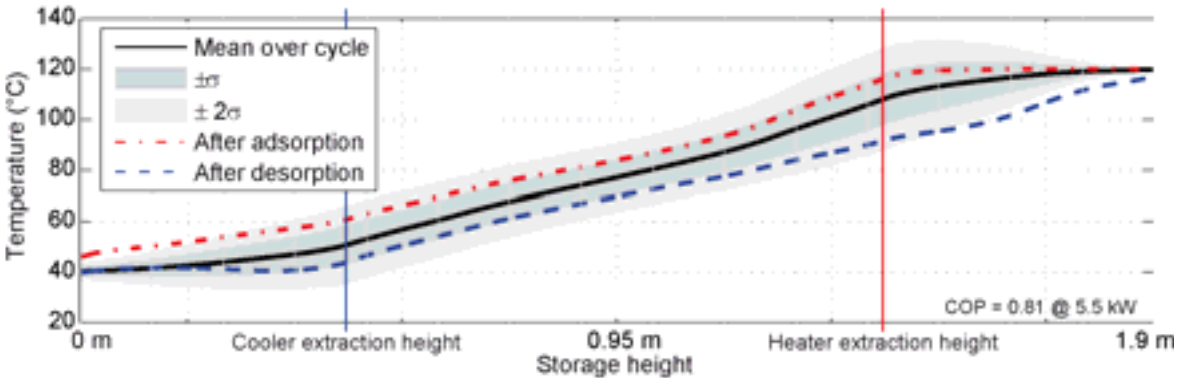

Fig. 5: Storage temperature profile over storage height, averaged over a full cycle (central line) as well as after adsorption phase (top line) and after desorption phase (bottom line).

More details about the stratification of the storage over the cycle are revealed by Fig. 6. For this evaluation, the storage has been divided numerically into 15 zones, with each solid line representing the average temperature of one zone. The dashed lines show the temperatures of the fluid entering and leaving the adsorber, and the fluid entering the heater and cooler. It can be seen how hot fluid at the top of the storage and cold fluid at its bottom are accumulated (through the operation of heater and cooler) until needed towards the end of the respective half-cycle. The intermediate zones of the storage are almost unaffected by the heater and cooler, their function is purely to store heat from the adsorber until needed for the next desorption. The adsorber inlet temperature T_{in} shows a characteristic sawtooth pattern as a result of the switching of extraction rings. The temperature profiles of the heater and cooler inlet show the superposition of the continuous operation of heater/cooler and the periodic visiting of the adsorber loop. The heater and cooler are treated as ideal here in the sense that they always supply 120 °C and 38 °C to the storage, respectively, independent of the required power (at constant mass flow). In this case, the power of heater und cooler fluctuates quite strongly over the cycle. If a more constant power demand on heater and cooler was desired, the buffer zones of the heater and cooler could be enlarged (either by moving their extraction heights towards the center of the storage or by increasing the storage volume). For the solar cooling application, the current heater operation scheme should be replaced by a ‘matched flow’ of the collector loop with the mass flow rate depending on collector insolation and temperature at the top of the storage.

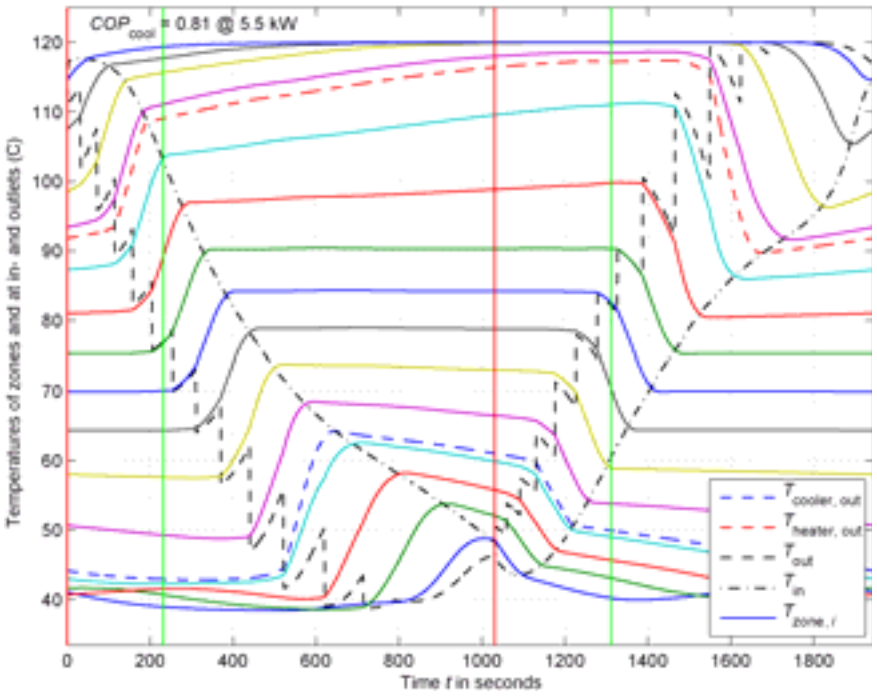

Fig. 6: Temperature variations in the storage over the cycle (same conditions as in Figures 4 and 5). The red vertical lines show the beginning of half cycles, the green vertical lines the end of the isosteric phases (as in Fig. 4).

Power control

The cooling power can be controlled through the adsorber mass flow, see Fig. 7. The mass flows in the heater and cooler loop are scaled to remain each at 35% of the adsorber mass flow. The tradeoff between COP and power in the Stratisorp cycle can be clearly seen here. For decreasing mass flow, the COP increases as the driving temperature differences in the adsorber are reduced and thus heat recovery is improved. However, there is a sharp maximum of the COP at some low mass flow. Below this value, the cycle time is increased so strongly that storage losses dominate.

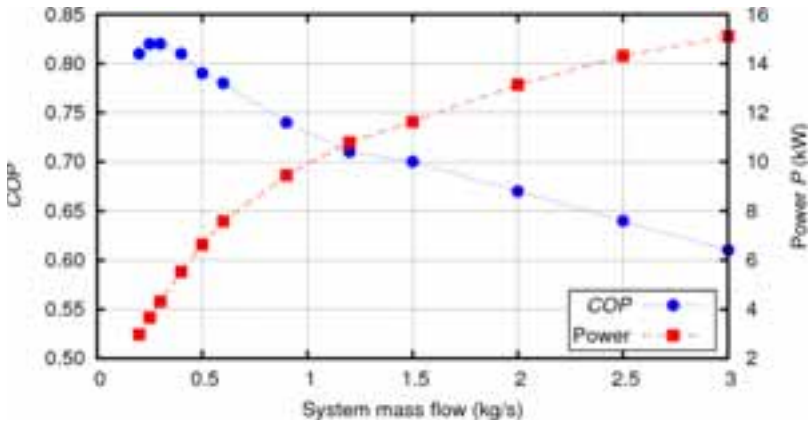

Fig. 7: COP and power of simulated Stratisorp system for as a function of adsorber mass flow. Temperatures are 120 °C (regeneration), 18 °C (evaporator supply), and 38 °C (condenser/adsorber cooling supply).

The design power of 10 kW is reached at a system mass flow of 1.0 kg/s with a COP of 0.73. If a high COP is not of paramount importance, the power can be increased further to 15 kW at a mass flow of 3 kg/s and a COP of 0.61. It should be noted, however, that auxiliary energy consumption for pumps and fans has been neglected in this analysis and is expected to play a very significant role at high mass flows. It should also be noted that operating parameters have not been adjusted or even optimized for each mass flow, so small improvements of COP and/or power could be expected from careful adjustment of ΔT_{set}.as well as the half-cycle switching criterion and the relative heater and cooler flow rates.

Variation of external temperatures

For the solar cooling application, which relies on the utilization of the storage as a buffer for solar energy from the collector, it is of high interest to see how the Stratisorp system reacts to a variation in driving temperature. From the base operating condition discussed in the previous section, the heater temperature T_{reg} is now varied between 70 °C and 130 °C (Fig. 8). The results are shown for two different system mass flows: 0.4 kg/s (as in Figures 4–6) denoted with subscript 'low' and 1.0 kg/s denoted with subscript 'high'.

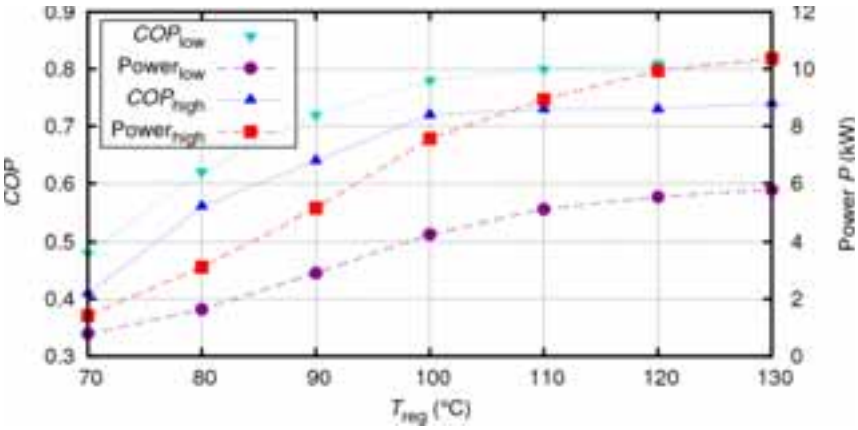

Fig. 8: COP and power of simulated Stratisorp system for stationary external temperatures: Variation of regeneration temperature for evaporator supply at 18 °C and condenser/adsorber cooling supply at 38 °C.

It can be seen that even with a required temperature lift of more than 20 K between evaporator supply (18 °C) and cooling tower supply (38 °C), the system is able to operate with driving temperatures as low as 70 °C, albeit at a low COP (0.48 and 0.41 at low/high power) and at a low power (0.8 kW and 1.4 kW). This means that the storage can be cooled at least down to this level by driving the cycle after heat supply from the collector has stopped. In this way, the heat losses of the storage over night can be strongly reduced. Obviously, this operation mode may require a cold storage depending on the cooling load profile.

At increasing regeneration temperature, the COP rises steeply up to values of 0.78 and 0.72 (low/high power) at 100 °C. At still higher temperatures, the cooling power continues to rise due to a higher mean driving temperature difference in the desorption phase, but the COP rises only marginally. Temperatures higher than 130 °C have not been considered here since for water as a storage fluid, high pressures are required to prevent boiling and thus safety requirements for steam boilers have to be observed.

Results on the variation of the evaporator supply temperature from the same base setting as before are shown in Fig. 9, again for high power (system mass flow 1.0 kg/s) and low power (0.4 kg/s). It can be seen that both COP and power vary almost linearly with evaporator temperature.

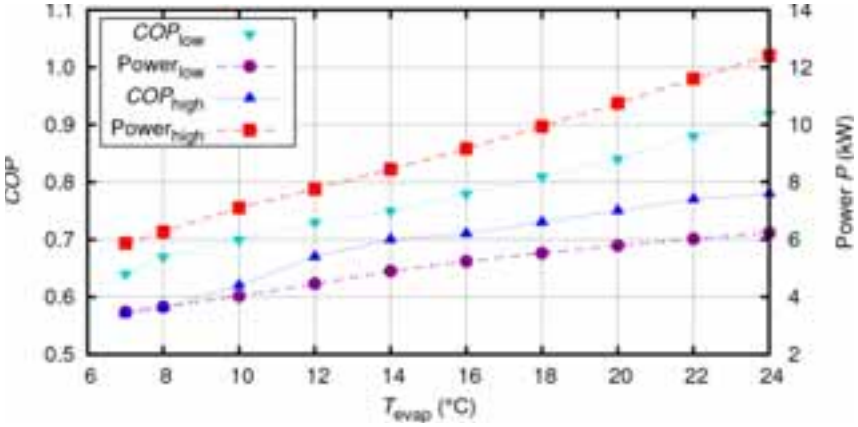

Fig. 9: COP and power of simulated Stratisorp system for stationary external temperatures: Variation of evaporator supply temperature for regeneration at 120 °C and condenser/adsorber cooling supply at 38 °C.

It can be seen that even at an evaporator supply temperature of 7 °C, COP values of 0.64 (at 3.5 kW) and 0.57 (at 5.9 kW) can be achieved. Thus, the system would be suitable for the operation of fan coils for air dehumidification if required. At very high evaporator temperatures, the COP values continue to rise since the recoverable heat is still increased.

Finally, results of a variation in heat rejection temperature are shown in Fig. 10. Again, the large possible operating range of this cycle can be seen. In this figure, two additional curves have been included for the low mass flow (0.4 kg/s), which correspond to an improved adsorber ('opt') with a higher adsorbent mass fraction in the composite and an increased thickness of the composite layer on the fluid channels. It can be seen that this change would increase both power (by about 1 kW on average) and COP (by a value of about 0.05 on average, with larger values at extreme temperatures).

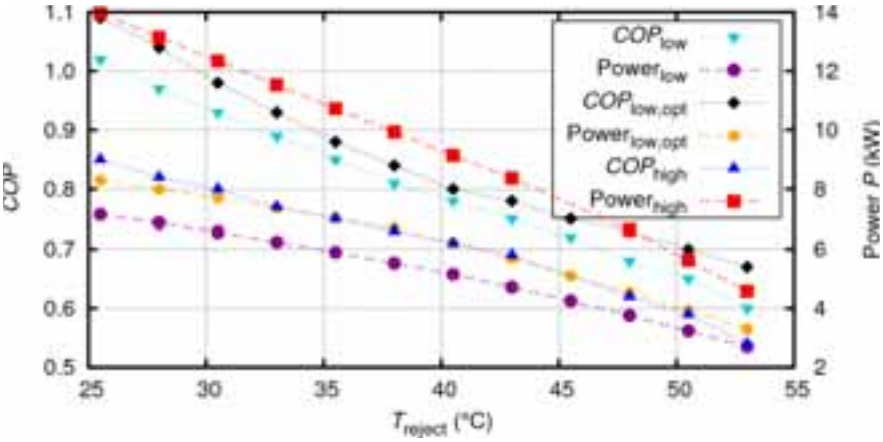

Fig. 10: COP and power of simulated Stratisorp system for stationary external temperatures: Variation of condenser/adsorber cooling supply for evaporator supply 18 °C and regeneration at 120 °C.

With the standard adsorber, even at air temperatures of 53°C, the system would be able to operate and achieve a COP of 0.54 (at 4.6 kW) or 0.6 (at 2.7 kW). Thus a dry cooling tower could be used even in hot climates. At decreasing air temperatures, both COP and power increase, with an increasing difference in COP between the two different mass flows. At 28 °C air temperature, the COP values are 0.97 (at 6.9 kW) and 0.82 (at 13.2 kW). Again, it is seen that the COP can reach very high values at a low temperature lift under part load conditions, since the overlap between the adsorption and desorption heat curves and thus the recoverable heat increases.

6. Conclusion and outlook

The Stratisorp cycle has been presented and dynamic system simulation results have been discussed under conditions relevant to solar cooling applications. We hope to have demonstrated that the cycle shows quite promising properties for this application. The next step would be a full transient simulation of a solar cooling system with fluctuating heat input from a collector and a fluctuating load from a building. Some basic ideas regarding an applicable control strategy have been given (matched flow for collector and adsorber mass flow control to match load), but we have not yet achieved a clean and robust implementation of such control strategy. It is also still an open question whether a larger buffer storage on the hot side should preferably be integrated into the Stratisorp storage or be kept separately from it.

We also hope to have shown that there still is a large potential to develop improved adsorption cycles and machines so that in a solar energy future, the niche for adsorption systems may be larger than commonly expected.

7. Acknowledgements

The authors received financial support via the Shared Research Group 2-03 funded by the Concept for the Future of Karlsruhe Institute of Technology within the framework of the German Excellence Initiative. We also gratefully acknowledge funding through the BWPlus programme of the Ministry of Environment and Transport of the state of Baden-Württemberg.

8. References

Andersen, E., Furbo, S., Hampel, M., Weidemann, W. and Müller-Steinhagen, H., 2008. Investigations on stratification devices for hot water heat stores. Int. J. Energy Res. 32, 255–263.

Cerkvenik, B., Poredos, A. and Ziegler, F., 2001. Influence of adsorption cycle limitations on the system performance. Int. J. of Refrigeration 24, 475–485.

Füldner, G., Schnabel, L., Wittstadt, U., Henning, H.-M. and Schmidt, F.P., 2011. Numerical layer optimization of aluminum fibre/SAPO-34 composites for the application in adsorptive heat exchangers. In: Proc. International Sorption Heat Pump Conference (ISHPC11), 6.–8.4.2011, Padua, Italy, pp. 533–542.

Henning, H.-M., 2007. Solar assisted air-conditioning of buildings – an overview. Applied Thermal Engineering 27, 1734–1749.

Kakiuchi, H., Shimooka, S., Iwade, M., Oshima, K., Yamazaki, M., Terada, S., Watanabe, H. and Takewaki, T., 2005. Water Vapor Adsorbent FAM-Z02 and Its Applicability to Adsorption Heat Pump, KAGAKU KOGAKU RONBUNSHU 31, 273–277.

Munz, G., Schmidt, F.P., Nunez, T. and Schnabel, L., 2009. Adsorption Heat Pump with Heat Accumulator. US Patent Application US 2009/0282846 A1.

Núñez, T., Henning, H.-M. and Mittelbach, W., 1999. Adsorption cycle modeling: characterization and comparison of materials. ISHPC'99, Proc of the 1999 Sorption Heat Pump Conf, München, Germany 24–26 March, Ebenhausen, Langewiesche/Brandt, p. 209.

Schmidt, F.P, Füldner G., Schnabel, L. and Henning, H.-M., 2007. Novel cycle concept for adsorption chiller with advanced heat recovery utilising a stratified storage. In: Proc. 2nd International Conference Solar Air-Conditioning, 18.–19.10.2007, Tarragona, Spain, pp. 618–623.

Schwamberger, V., Joshi, C. and Schmidt, F.P., 2011. Second law analysis of a novel cycle concept for adsorption heat pumps. In: Proc. International Sorption Heat Pump Conference (ISHPC11), 6.–8.4.2011, Padua, Italy, pp. 991–998.

Schwamberger, V., Glück, C., Joshi, C. and Schmidt, F. P., 2011a. A novel adsorption cycle with advanced heat recovery for high efficiency air-cooled adsorption chillers. In.: Proc. 23rd IIR Int. Congress of Refrigeration, August 21–26, Prague, Czech Republik.

Wittstadt, U., Füldner, G., Schnabel, L., Schmidt F., 2009. Comparison of the heat transfer characteristics of two adsorption heat exchanger concepts. In: Proc. of the Heat Powered Cycles Conference, September 7–9, 2009, Berlin, Germany, ISBN 978-0-9563329-0-5.